Determination of Surface Coverage and Orientation of Reduced Cytochrome *c* on a Silica Surface with Polarized ATR Spectroscopy

Casey M. Kraning, Tara L. Benz, Kayla S. Bloome, Gregory C. Campanello, Victoria S. Fahrenbach, Sheetal A. Mistry, Carrie Ann Hedge, Ken D. Clevenger, Keith M. Gligorich, Todd A. Hopkins,*,† Geoffrey C. Hoops, Sergio B. Mendes,‡ Huan-Cheng Chang,§ and Meng-Chih Su⊥

Department of Chemistry, Butler University, 4600 Sunset Avenue, Indianapolis, Indiana 46208, Department of Physics and Astronomy, University of Louisville, Louisville, Kentucky 40292, Institute of Atomic and Molecular Sciences, Academia Sinica, P.O. Box 23-116, Taipei, Taiwan 106, Republic of China, and Department of Chemistry, Sonoma State University, Rohnert Park, California 94928

Received: March 8, 2007; In Final Form: June 18, 2007

Linearly polarized attenuated total internal reflection (ATR) spectroscopy is used to study the adsorption properties of reduced cytochrome *c* to a silica surface. The adsorption equilibrium constant, surface coverage, protein orientation, effect of NaCl, and pH dependence are determined for the adsorption of reduced cytochrome *c* onto a silica surface. Surface coverage results (at pH 7.2) show that reduced cytochrome *c* packs onto the silica surface at <80% of a closely packed monolayer. The protein orientation distribution as measured by an order parameter is shown to be dependent on the surface coverage and solution pH. All of the results for the surface adsorption of reduced cytochrome *c* on silica are indicative of an electrostatically driven interaction. The results for reduced cytochrome *c* are compared to surface adsorption results for oxidized cytochrome *c* on silica. These results indicate that there is no significant difference in the adsorption behavior correlating to the oxidation state of this heme protein.

Introduction

Protein adsorption to solid surfaces is a topic of considerable interest, because of its importance in biosensors, chromatography, biocompatibility, and many biotechnology applications. Understanding of surface adsorption properties of proteins and characterization of protein thin films are critical to the further development of many of these technologies. Attenuated total internal reflection (ATR) spectroscopy has proven to be a useful tool for studying proteins adsorbed to a variety of surfaces.[1−8] In ATR measurements, the limited penetration of the evanescent wave provides information about proteins confined to the surface without interference from proteins in the bulk solution. It provides a direct measure of the surface coverage along with an indication of any conformational changes that occur.[1] Utilizing polarized ATR spectroscopy allows for the determination of an order-parameter of the molecular orientation of surface-bound proteins. This technique has been especially useful for studying the adsorption behavior of heme-containing proteins.[1−8]

Cytochrome *c* is a globular protein with well-characterized structural and spectroscopic properties.[9] It functions as a redox protein that utilizes a change in the oxidation state of the iron at the center of the heme group for electron transfer. Oxidized cytochrome *c* is characterized by iron in a +3 state (ferric) and reduced cytochrome *c* has iron in a +2 state (ferrous), and NMR structures exist for each oxidation state of the protein.[10,11] The heme absorbance spectra of reduced and oxidized proteins show α, β, and Soret band (γ) spectroscopic features that are characteristic of and provide a means of monitoring the oxidation state of the protein.[12] Under near-neutral pH conditions, cytochrome *c* is positively charged, which provides an electrostatic driving force for its adsorption to negatively charged surfaces (e.g., phospholipid membranes, tin oxide, and silica).

Cytochrome *c* has proven to be an ideal prototype protein for adsorption studies to a host of different surfaces, including (but certainly not limited to) silica oxynitride,[13] silica,[1] gold,[14] and others.[15,16] However, the majority of studies of cytochrome *c* adsorption properties are limited to the oxidized form of cytochrome *c*. Even in studies following the electrochemical properties of films of cytochrome *c*, the oxidized form is used in the adsorption process, and then an electric potential is used to change the oxidation state of the adsorbed protein.[17−19] One notable exception is a comparison study of the adsorption of both oxidized and reduced cytochrome *c* to a tin oxide electrode.[20] Even in that study the results for reduced cytochrome *c* on tin oxide were considered "problematical" by the authors.[20] Therefore, the objective of this research effort is to obtain an understanding of the adsorption properties of reduced cytochrome *c* to a silica surface, which is a model negatively charged surface. One of the goals of the study is to provide a basis for comparison with electrostatically driven adsorption of oxidized cytochrome *c*.

In this study, ATR spectroscopic measurements are utilized to study the adsorption of reduced cytochrome *c* to a silica surface. Adsorption isotherms are characterized for both oxidation states of the protein, using the strong Soret absorption band of reduced (~416 nm) and oxidized cytochrome *c* (~409 nm) in ATR measurements. The effect of ionic strength, specifically

* Address correspondence to this author. E-mail: tahopkin@butler.edu.
† Butler University.
‡ University of Louisville.
§ Academia Sinica.
⊥ Sonoma State University.

10.1021/jp071896y CCC: $37.00
Published on Web 08/15/2007

NaCl, on the adsorption isotherms of reduced cytochrome *c* to silica is investigated. The polarized ATR measurements are used to determine an order-parameter for the orientation of surface-bound reduced cytochrome *c*, the surface coverage, and adsorption equilibrium constants for reduced cytochrome *c* on the silica surface. These results are compared with results from the adsorption of oxidized cytochrome *c* on silica, and the similarities are discussed. The pH dependence of both surface coverage and order parameter is also investigated for reduced cytochrome *c* on silica surface.

Experimental Section

Oxidized Cytochrome *c* Preparation. Horse heart cytochrome *c* was obtained commercially (Sigma) and used without further purification. It was dissolved in deionized water to give an approximate concentration of 1 mM. The protein was injected into a dialysis cassette (Pierce) and dialyzed in an autoclaved 10 mM NaCl solution at 5 °C for ~20 h. The concentration of the stock was then determined spectroscopically, using the molar absorptivity coefficient of the Soret peak of oxidized cytochrome *c* ($\epsilon_{408} = 1.06 \times 10^5\ M^{-1}\ cm^{-1}$).[21] For the oxidized cytochrome *c* adsorption studies, the stock solution was diluted to concentrations in the 0.1−200 μM range, using phosphate buffer (7 mM) at pH 7.2. For pH dependence studies, the stock solution was diluted with 7 mM phosphate buffer for (pH 3.75 and >4.75) and 7 mM succinate buffer for pH 4.00−4.75.

Reduced Cytochrome *c* Preparation. The ~1 mM oxidized cytochrome *c* stock solution was reduced with sodium dithionite (0.29 M) at room temperature in phosphate buffer (3 mM) at pH 7. The reduced protein was immediately purified by size exclusion chromatography (Sephadex G-25 in 10 mM phosphate buffer, pH 7.0, under inert N_2 atmosphere). To maintain the reduced state, 1 mM L-ascorbic acid was added to the cytochrome *c* stock solution. The reduced stock solution was stored under an inert N_2 atmosphere at 4 °C, and the concentration was determined spectroscopically, using the molar absorptivity coefficient of the Soret peak of reduced cytochrome *c* ($\epsilon_{416} = 1.29 \times 10^5\ M^{-1}\ cm^{-1}$).[22] For the reduced cytochrome *c* adsorption studies, the reduced stock solution was diluted to concentrations in the 0.1−60 μM range, using phosphate buffer (7 mM) with and without 150 mM NaCl at pH 7.2. L-Ascorbic acid was added to each sample to a final concentration of 1 mM. For pH dependence studies, the stock solution was diluted with 7 mM phosphate buffer for pH 3.75 and >4.75 and 7 mM succinate buffer for pH 4.00−4.75. All samples were analyzed within 1 h of preparation to prevent oxidation during the study. However, under the conditions described here, the samples were later found to maintain their reduction for at least 1 month when kept tightly capped at 4 °C.

ATR Spectroscopy. The face of a right-angle fused silica prism (CVI) served as the silica surface for cytochrome *c* adsorption. The surface has a specified flatness of $\lambda/10$ (λ = 633 nm) and was used as received. Prior to use, the prism was thoroughly cleaned with standard cleaning solutions, rinsed extensively with deionized water, and dried with methanol.

The absorption spectra over the 300−700 nm wavelength range of free and surface-bound protein molecules were acquired with a UV−vis spectrophotometer (Cary 50). A fused silica prism in a single-pass ATR arrangement was used for the measurement of the surface-bound proteins. The prism was inserted into the compartment of the spectrophotometer in a manner similar to that of the solution sample cell. In the ATR measurement, the evanescent wave detected the adsorbate via the internal reflection of the light through the right-angle prism on which a static sample cell was situated. The sample cell was made of a modified rubber O-ring (~26 mm diameter), separating the prism from a glass plate. This assembly was held in place by a custom-made stainless steel mounting block. The space (~0.5 mL) created by the O-ring was filled with the sample solution in the individual measurements. To ensure that the protein surface adsorption had reached equilibrium before collecting ATR spectra, the Soret absorbance was monitored during sample introduction. After the absorbance reached a constant and maximum level (typically <5 min), ATR spectra were acquired.

Linear dichroism spectra were measured with a dichroic polarizer (Bolder Vision Optik), which has a manufacturer-specified extinction ratio of 2.5×10^{-3} over the 400−430 nm wavelength range (i.e., Soret absorption range). The polarizer was mounted on a rotary precision stage (Thor Labs) for selection of the light polarization (TE- or TM-polarized). For each ATR sample, 5 nonpolarized spectra and 12−17 of each polarized spectra were acquired. All of the absorption spectra were collected at room temperature. For any single adsorption isotherm (e.g., variable reduced cytochrome *c* concentration, 7 mM phosphate data), the prism was held in a constant position with respect to the incident radiation in order to ensure that the same surface location was probed for each measurement.

The ATR cell was cleaned following the removal of each protein sample with a series of five washes: 1 wash with 1% (w/v) SDS detergent for ~30 s, 1 wash with acidic water (pH 3−4) for ~15 s, 2 washes with basic water (pH 8−9), followed by a wash with autoclaved 7 mM phosphate buffer (pH 7.2) for ~30 s. The buffer wash was used for baseline scans. Following the wash procedure, the concentration of adsorbed cytochrome *c* on the prism was below spectroscopic detection limits.

Data Analysis. The ATR spectra for each polarization were averaged together and smoothed with a 2-point moving average. Because of the relatively small signal, the averaged and smoothed ATR spectra were then fitted with a solution spectrum to determine the location and absorbance of the Soret band. The fitting solution spectrum was chosen based on the clarity of the absorbance of its Soret band and the presence of a relatively flat reference baseline in the 600−700 nm region where no absorbance is observed. The observed spectroscopic structure and band shapes are identical for solution and ATR surface spectra. The fitting solution spectrum is taken under the same solution conditions as the ATR data to be analyzed, and is typically from the higher end of the cytochrome *c* concentration range. The fitting solution spectrum is overlaid onto the averaged and smoothed ATR spectrum, so that its baseline bisects the noise in the 600−700 nm range, and it fits the maximum absorbance value of the ATR spectra. For particularly noisy spectra, especially polarized spectra, an upper and lower limit of absorbance were determined by adjusting the fitting solution spectrum to enclose the upper and lower portions of the noise in the Soret band ignoring random large noise peaks. These two spectra were averaged to determine wavelength and absorbance values.

Theory Section

For treating our polarized ATR data we employed the theoretical formalism described in ref 5, which combines a rigorous transfer-matrix calculation and a Kramers−Kronig transformation to determine in a self-consistent manner the real and imaginary parts of the refractive index, the surface coverage, and the second-order orientation parameter of a surface-adsorbed

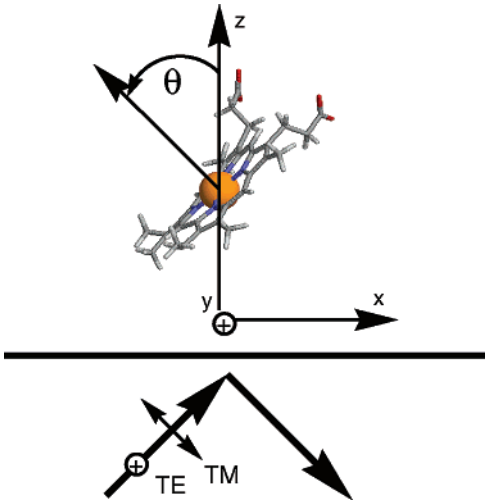

Figure 1. Schematic showing the angle, θ, between the normal to the heme group and the surface normal, coordinate system, and polarization of the incident light beam. The structure of the heme is adapted from ref 11.

protein film. The adopted Cartesian coordinate system is defined in Figure 1 with the plane of incidence of the light beam in the $x-z$ plane, and therefore the electric field in the TE polarization has only a y-component and in the TM polarization it has components along the x and z axis. The sample (film/prism) surface is then the $x-y$ plane.

As described in detail in ref 5, TE polarized absorbance data are considered first because it involves only the y-component of the complex refractive index. The real part of the refractive index of the protein film along the y axis (n_y) is initially estimated, and the value for k_y is iteratively varied to match the calculated and experimental absorbances. Next, TM absorbance data are considered, where the calculations involve both x and z components of the complex refractive index. However, for films that are randomly adsorbed from a bulk phase we can assume in-plane symmetry for the optical constants, which allow us to write $n_x = n_y$ and $k_x = k_y$. Then a value for the real portion of the refractive index along the z axis (n_z) is estimated and a value for k_z that matches the calculated and experimental absorbances is iteratively determined. Once the imaginary parts of the refractive index along each Cartesian axis are determined, then the surface coverage (Γ) can be calculated through the following relation:[5]

$$\Gamma = \frac{4\pi(k_x + k_y + k_z)t}{3\epsilon\lambda \ln(10)} \tag{1}$$

where ϵ is the molar absorptivity of the dissolved molecule and t is the thickness of the layer defined by the linear dimension of the protein. The real portion of the refractive index of this layer depends on the solute and solvent concentration in the layer. For the adsorbed cyt c films examined here, we have used the surface coverage obtained from eq 1, the molar absorptivity of cytochrome c measured over a broad spectral range, and a Kramers−Kronig relation to refine the initial estimate for the real part of the refractive index along each Cartesian axis, n_γ, with $\gamma = x, y, z$. Once refined n_γ values are determined, the previously described routine is repeated to generate new refined values of k_γ and Γ, which are used to further refine values of n_γ. This iterative process typically converges in 2−5 loops.

Once the dichroic values of the imaginary part (k_x, k_y, and k_z) have been obtained, then an average molecular orientation described by $\langle\cos^2\theta\rangle$ can be determined. In the case of

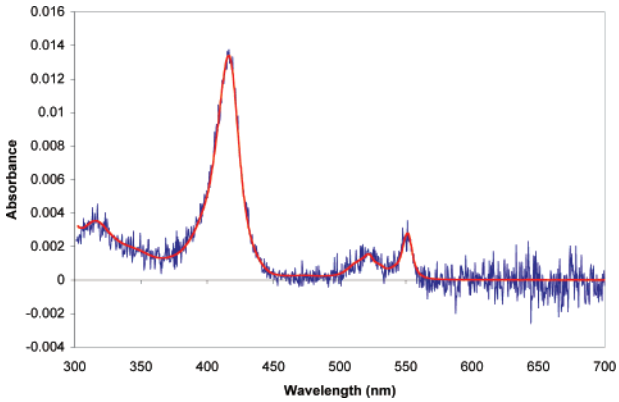

Figure 2. Nonpolarized ATR absorbance spectra of reduced cytochrome c adsorbed to a silica surface from 5.77 μM reduced cytochrome c, pH 7.2, 7 mM phosphate, 1 mM ascorbic acid. Noisy blue spectrum is the average of 5 scans with 2-point smoothing, and the smooth red line is a fit to the data using a solution spectrum.

cytochrome c with two orthogonal dipoles in the heme plane, which defines a circular absorber, we have[5]

$$\langle\cos^2\theta\rangle = 1 - \frac{2k_z}{k_x + k_y + k_z} \tag{2}$$

where θ is the angle between the normal to the heme plane and the z axis. The second-order parameter is then calculated by

$$\langle P_2(\cos\theta)\rangle = \frac{3}{2}\langle\cos^2\theta\rangle - \frac{1}{2} \tag{3}$$

Results and Discussion

Adsorption Isotherms. Figure 2 shows an example of a nonpolarized ATR absorbance spectrum of reduced cytochrome c adsorbed to a silica surface from a 5.77 μM bulk solution concentration at pH 7.2. The Soret (γ) band location at 416 nm and the sharp α band at 550 nm are indicative of reduced cytochrome c (i.e., Fe^{2+}), whereas the Soret band shifts to ca. 409 nm and the α band broadens into the β band (520 nm) in the oxidized form of cytochrome c. Therefore, the ATR spectra can be used to monitor the oxidation state of the heme iron as well as the concentration and orientation of cytochrome c on the silica surface. The shape and location of the spectra were monitored for evidence of oxidation over the course of these experiments. The addition of 150 mM NaCl did not change the location or shape of the spectral features of cytochrome c (spectrum not shown).

Figure 3 shows adsorption isotherms of reduced cytochrome c on fused silica with (150 mM) and without NaCl. The adsorption isotherms are plots of ATR absorbance (Soret band ~416 nm) vs bulk solution reduced cytochrome c concentration. The cytochrome c concentration spans 0−60 (no NaCl) and 0−100 μM (150 mM NaCl). Each of the data sets shown were fit to a Langmuir adsorption model

$$A = \frac{K_{ad} A_{sat} C_b}{1 + K_{ad} C_b} \tag{4}$$

where A is the absorbance, K_{ad} is the adsorption equilibrium constant, A_{sat} is the absorbance upon saturation of the surface (i.e., all adsorption sites are occupied), and C_b is the concentration in bulk solution. The data in Figure 3 fit reasonably well to the Langmuir adsorption model in eq 4, and the values of the equilibrium constants are $K_{ad} = 1.0 \times 10^7$ M^{-1} (no NaCl) and 4.0×10^5 M^{-1} (150 mM NaCl). Comparison of the

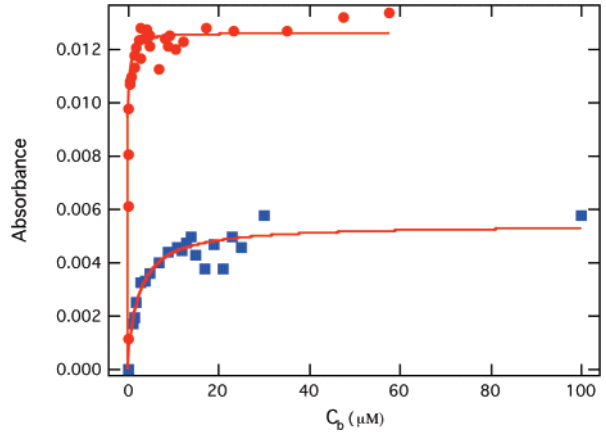

Figure 3. Adsorption isotherms (ATR absorbance vs bulk concentration (C_b)) of reduced cytochrome *c* on fused silica. Each sample is pH 7.2, 7 mM phosphate buffer, 1 mM ascorbic acid with 150 mM NaCl (squares) and without (circles). The solid lines represent Langmuir fits (eq 1) to the data.

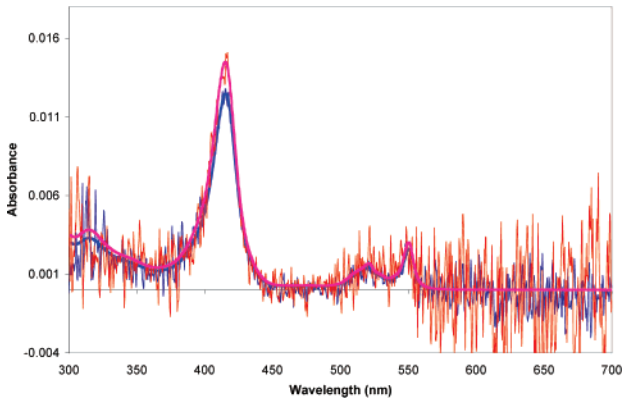

Figure 4. Polarized ATR absorbance spectra for reduced cytochrome *c* adsorbed to a silica surface under solution conditions: 5.77 μM reduced cytochrome *c*, pH 7.2, 7 mM phosphate, 1 mM ascorbic acid. Noisy blue spectrum is TM polarized data, and the smooth blue spectrum is the fit to these data. Noisy red spectrum is TE polarized data, and the smooth red spectrum is the fit to these data using a solution spectrum.

isotherms shows that the presence of 150 mM NaCl results in a decrease of A_{max} by a factor of 2 and a decrease of K_{ad} by a factor of 20. Under these experimental conditions (pH 7.2) the interaction between cytochrome *c* (positively charged) and the silica surface (negatively charged) is primarily electrostatic, and the results with additional NaCl are consistent with an ionic strength mediated interaction between cytochrome *c* and the silica.

Surface Coverage and Orientation. Figure 4 shows the polarized ATR absorbance spectrum of reduced cytochrome *c* adsorbed to fused silica from a 5.77 μM concentration bulk solution. As described in the Theory Section, the TE and TM polarized data (as shown in Figure 4) were used in our calculations to determine the surface coverage (Γ) and the order parameter, $\langle P_2(\cos\theta)\rangle$, of reduced cytochrome *c* adsorbed to silica.

Figure 5 shows plots of the surface coverage of reduced cytochrome *c* on a silica surface with and without 150 mM NaCl. With no NaCl added, the maximum surface coverage is $\Gamma = 18$ pmol/cm^2, which is around 3 times the maximum surface coverage with 150 mM NaCl. On the basis of the crystallographic dimensions of the protein,[5] a close-packed monolayer of cytochrome *c* would have a surface coverage of ca. 22 pmol/cm^2. Therefore, even at the lowest ionic strength, the thin film

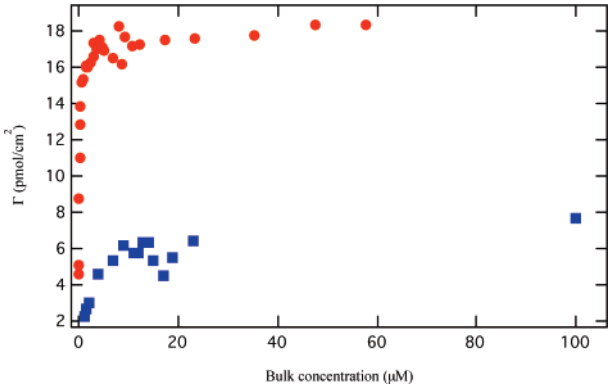

Figure 5. Plots of surface coverage vs bulk concentration (adsorption isotherms) for reduced cytochrome *c* adsorbed to a silica surface at pH 7.2, 7 mM phosphate, 1 mM ascorbic acid: 0 (circles) and 150 mM (squares) NaCl.

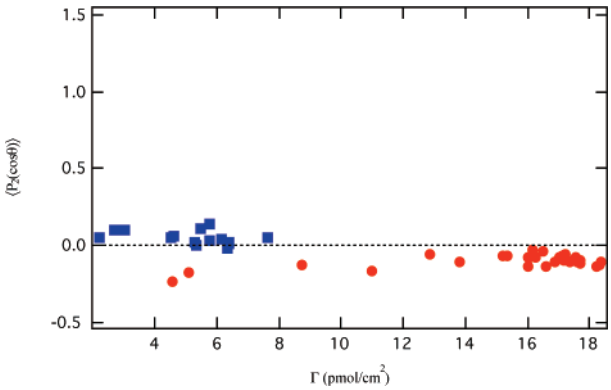

Figure 6. Plots of the order parameter, $\langle P_2(\cos\theta)\rangle$ vs surface coverage of reduced cytochrome *c* on silica, pH 7.2, 7 mM phosphate, 1 mM ascorbic acid: 0 (circles) and 150 (squares) mM NaCl. The dashed line is included to show $\langle P_2(\cos\theta)\rangle = 0$.

of reduced cytochrome *c* is no more than 80% of a monolayer on a silica surface. Collinson and Bowden measured adsorption isotherms for reduced cytochrome *c* adsorbed to tin oxide electrodes,[20] which is also dominated by electrostatic interactions. This study reported saturation surface coverages of $\Gamma \approx 18$ pmol/cm^2 at pH 7.0, 10 mM phosphate, and $\Gamma = 6.8$ pmol/cm^2 at pH 7.0, 150 mM phosphate.[20] The results on tin oxide are almost identical with the results in Figure 5 even though NaCl was used for ionic strength in this study instead of potassium phosphate.

Figure 6 shows how the order parameter, $\langle P_2(\cos\theta)\rangle$, of reduced cytochrome *c* adsorbed to a silica surface varies with surface coverage for both, with and without NaCl. The data in Figure 6 show a small but distinct NaCl dependence to the order parameter. With no NaCl, the order parameter is slightly negative, ca. -0.10, where it is slightly positive, $\sim$0.05, with 150 mM NaCl. These measured order parameters, while small, are nonzero, which indicates that the protein orientation distribution is not completely random. Figure 6 also shows a difference in the surface coverage dependence of the order parameter. The order parameter for the 0 mM NaCl data gets more negative (ca. -0.20) at surface coverage <6 pmol/cm^2, which indicates a more ordered protein film at the lowest surface coverages. This contrasts with the 150 mM NaCl data, which show no change in the order parameter down to surface coverage <4 pmol/cm^2.

pH Dependence. The pI of cytochrome *c* is $\sim$10.5 and the pK_a of silica is ca. 2$-$3, which means that there is a favorable electrostatic interaction between pH 3 and 10.5. Figure 7 shows

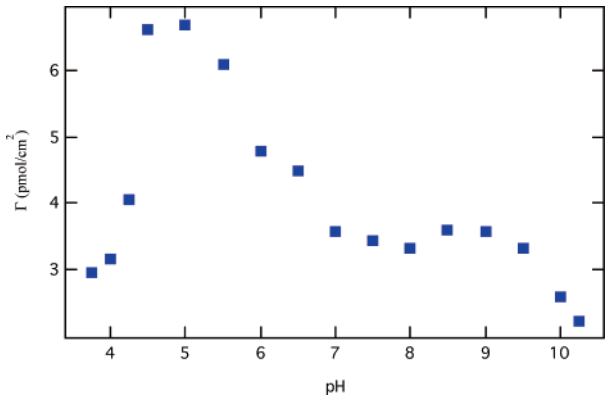

Figure 7. Surface coverage vs pH for reduced cytochrome *c* adsorbed to a silica surface from 1 μM cyt *c*, 7 mM phosphate (or succinate), 1 mM ascorbic acid, 150 mM NaCl solution.

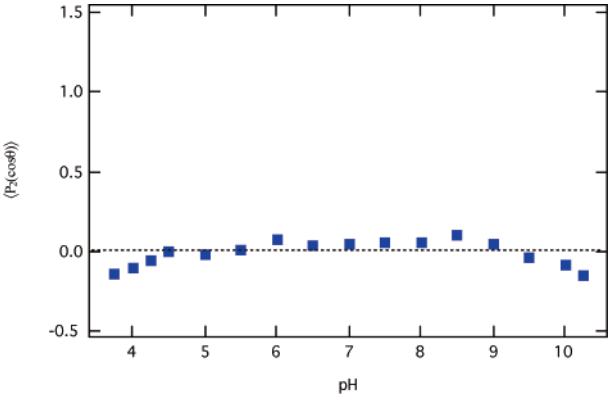

Figure 8. Plot of the order parameter, $\langle P_2(\cos\theta)\rangle$, vs pH for reduced cytochrome *c* adsorbed to a silica surface from 1 μM cyt *c*, 7 mM phosphate (or succinate), 1 mM ascorbic acid, 150 mM NaCl solution. The dashed line is included to show $\langle P_2(\cos\theta)\rangle = 0$.

the pH-dependent surface coverage of reduced cytochrome *c* from a 1 μM solution containing 150 mM NaCl, over the pH range 3.75−10.5. The lowest pH data point recorded was above the pK_a of silica, because the reduced cytochrome *c* underwent oxidation at the silica surface below pH 3.75. No surface coverage was observed above pH 10.5 (∼pI of protein), because the interaction between the silica surface and protein is no longer electrostatically favorable.

The pH dependence of the order parameter of reduced cytochrome *c* adsorbed to silica is shown in Figure 8. Over the pH range 6−9, the order parameter is roughly constant, $\langle P_2(\cos\theta)\rangle \approx 0.05$, which corresponds to the average order parameter reported in Figure 6 for the 150 mM NaCl data. At the low (<5.5) and high (>9) pH ends, the value of $\langle P_2(\cos\theta)\rangle$ decreases to ca. −0.15. At the extremes of the pH range it is difficult to eliminate the possibility of a conformational change in the protein, which could cause the observed order parameter changes. Because of the dominance of electrostatic interactions, it is also reasonable to expect that at these pH values the orientation distribution of reduced cytochrome *c* on silica would be considerably different than that at near-neutral pH. From the measurements presented in this paper, it is not possible to say with certainty the cause of the pH dependence of the order parameter shown in Figure 8.

Comparison with Oxidized Cytochrome *c*. The adsorption of oxidized cytochrome *c* (i.e., Fe(III) in heme group) to silica has been investigated in a number of previous studies.[1−6] The surface coverages reported range from 11 to 22 pmol/cm^2 for solutions with 7−10 mM phosphate.[1,5] Because of the significant differences in reported values, an adsorption isotherm with

TABLE 1: Summary of Adsorption Isotherm Results for Reduced Vs Oxidized Cytochrome *c* on a Silica Surface.

bulk solution conditions	K_{ad} ($\times 10^{-6}$ M^{-1})[a]	$\langle P_2(\cos\theta)\rangle$[b]	Γ (pmol/cm^2)[c]
oxidized cyt *c*, pH 7.2, 7 mM phosphate	12 ± 2	−0.15	17
reduced cyt *c*, pH 7.2, 7 mM phosphate, 1 mM ascorbic acid	10 ± 1	−0.10	18
reduced cyt *c*, pH 7.2, 7 mM phosphate, 1 mM ascorbic acid, 150 mM NaCl	0.4 ± 0.07	0.05	6

[a] Adsorption equilibrium constant determined by fitting isotherm data to eq 4. [b] Values for order parameter are reported for saturated surface conditions only. The uncertainty in the order parameter is approximately 0.10. [c] Surface coverage values for saturated surface conditions only.

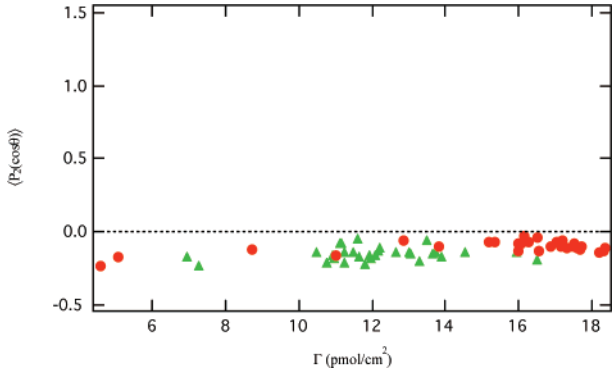

Figure 9. Plot of the order parameter, $\langle P_2(\cos\theta)\rangle$ vs bulk concentration for (red circles) reduced cytochrome *c* (pH 7.2, 7 mM phosphate, 1 mM ascorbic acid) and (green triangles) oxidized cytochrome *c* (pH 7.2, 7 mM phosphate) adsorbed to a silica surface. The dashed line is included to show $\langle P_2(\cos\theta)\rangle = 0$.

polarized ATR spectra was measured for oxidized cytochrome *c* (0−100 μM), pH 7.2, 7 mM phosphate buffer in order to compare with reduced cytochrome *c* surface adsorption under almost identical experimental conditions. Results from the adsorption isotherm of oxidized cytochrome *c* are presented in Table 1 along with a summary of the reduced cytochrome *c* adsorption results. The adsorption equilibrium constants, order parameters, and surface coverage are shown for oxidized and reduced (0 and 150 mM NaCl) cytochrome *c* on a silica surface. Comparison of the results shows that the K_{ad} (12×10^6 vs 10×10^6 M^{-1}) and $\langle P_2(\cos\theta)\rangle$ (−0.15 vs −0.10) are not significantly different for oxidized vs reduced cytochrome *c*. The surface coverage at saturation is ∼80% of a close-packed monolayer for both oxidized and reduced cytochrome *c* on silica.

For a more complete comparison, Figure 9 shows plots of the order parameter vs surface coverage for oxidized and reduced cytochrome *c* adsorbed to a silica surface. It is clear that the data in Figure 9 show more similarities than differences. The data show the same general surface coverage dependence in the order parameters for both oxidation states of the protein. The most significant difference between the data sets is that reduced cytochrome *c* reaches a larger maximum surface coverage. However, the amount of scatter in the individual data points makes it extremely difficult to derive quantitative conclusions from these comparisons. Even considering this uncertainty, the data provided in Table 1 and Figure 9 indicate that the oxidation state of cytochrome *c* plays little role in the adsorption properties of the protein on a silica surface.

It is important to note in this discussion that ATR measurements of the heme spectra in this study do not show any

evidence of conformation changes[23,24] in either oxidation state of the protein upon adsorption to silica. While previous studies[23,24] show that heme spectra are sensitive to conformational changes in cytochrome *c*, it is not a "global" measurement of protein structure. Therefore, it is impossible to say with absolute certainty that cytochrome *c* (reduced or oxidized) does not undergo any conformation change upon adsorption.

Conclusions

Polarized ATR measurements are used to measure adsorption isotherms, order parameters, surface coverage, and pH dependence of reduced cytochrome *c* adsorbed to a silica surface. The electrostatic nature of the protein−silica interaction is demonstrated in the ionic strength dependent isotherm and surface coverage results, which show large decreases in adsorption equilibrium constant and surface coverage (at surface saturation). Measurements of the order parameter indicate that there is surface coverage dependence and ionic strength (NaCl) dependence to the protein orientation distribution on silica. The ionic strength dependence of the order parameter of cytochrome *c* is currently being investigated in our laboratories. The pH dependence of reduced cytochrome *c* adsorption to silica confirms that the interaction is primarily electrostatic, and the order parameter measurements show that the orientation of reduced cytochrome *c* in a thin film on silica is consistent under near-neutral pH conditions (pH 6−9). At low and high pH conditions, surface adsorption decreases and the order parameter changes, which could signify either a difference in the protein orientation distribution at the surface or a conformational change of the protein. Comparison of the surface adsorption of reduced vs oxidized cytochrome *c* reveals good agreement for the adsorption equilibrium constants, surface coverage, and order parameters. This shows that the oxidation state of cytochrome *c* has little influence on its adsorption properties on a silica surface.

Acknowledgment. The authors would like to thank the Lilly Foundation and the Butler Institute of Research and Scholarship for financial contributions. S.B.M. acknowledges NSF support under grant DBI 0352449 and the contribution from Baylor C. Brangers for running the computer codes based on ref 5.

Supporting Information Available: Figures showing the adsorption isotherm for oxidized cytochrome *c* and ATR absorbance vs pH for reduced cytochrome *c* adsorbed to silica. This material is available free of charge via the Internet at http://pubs.acs.org.

References and Notes

(1) Cheng, Y. Y.; Lin, S. H.; Chang, H. C.; Su, M. C. *J. Phys. Chem. A* **2003**, *107*, 10687.

(2) Edmiston, P. L.; Lee, J. E.; Cheng, S.-S.; Saavedra, S. S. *J. Am. Chem. Soc.* **1997**, *119*, 560.

(3) Qi, Z.; Matsuda, N.; Takatsu, A.; Kato, K. *J. Phys. Chem. B* **2003**, *107*, 6873.

(4) Flora, W. H.; Mendes, S. B.; Doherty, W. J., III; Saavedra, S. S.; Armstrong, N. R. *Langmuir* **2005**, *21*, 360.

(5) Runge, A. F.; Rasmussen, N. C.; Saavedra, S. S.; Mendes, S. B. *J. Phys. Chem. B* **2005**, *109*, 424.

(6) Runge, A. F.; Mendes, S. B.; Saavedra, S. S. *J. Phys. Chem. B* **2006**, *110*, 6732.

(7) Du, Y.-Z.; Saavedra, S. S. *Langmuir* **2003**, *19*, 6443.

(8) Edmiston, P. L.; Lee, J. E.; Wood, L. L.; Saavedra, S. S. *J. Phys. Chem.* **1996**, *100*, 775.

(9) Pettigrew, G. W.; Moore, G. C. *Cytochromes c*: *Biological Aspects*; Springer-Verlag: Berlin, Germany, 1987.

(10) Banci, L.; Bertini, I.; Gray, H. B.; Luchinat, C.; Reddig, T.; Rosato, A.; Turano, P. *Biochemistry* **1997**, *36*, 9867.

(11) Banci, L.; Bertini, I.; Huber, J. G.; Spyroulias, G. A.; Turano, P. *JBIC, J. Biol. Inorg. Chem.* **1999**, *4*, 21.

(12) Lvov, Y.; Ariga, K.; Ichinose, I.; Kunitake, T. *J. Am. Chem. Soc.* **1995**, *117*, 6117.

(13) Walker, D. S.; Hellinga, H. W.; Saavedra, S. S.; Reichert, W. M. *J. Phys. Chem.* **1993**, *97*, 10217.

(14) Chah, S.; Kumar, C. V.; Hammond, M. R.; Zare, R. N. *Anal. Chem.* **2004**, *76*, 2112.

(15) Macdonald, I. D. G.; Smith, W. E. *Langmuir* **1996**, *12*, 706.

(16) Xu, W.; Zhou, H.; Regnier, F. E. *Anal. Chem.* **2003**, *75*, 1931.

(17) Hedges, D. H. P.; Richardson, D. J.; Russell, D. A. *Langmuir* **2004**, *20*, 1901.

(18) Petrovic, J.; Clark, R. A.; Yue, H.; Waldeck, D. H.; Bowden, E. F. *Langmuir* **2005**, *21*, 6308.

(19) Runge, A. F.; Saavedra, S. S. *Langmuir* **2003**, *19*, 9418.

(20) Collinson, M.; Bowden, E. F. *Langmuir* **1992**, *8*, 2552.

(21) Babul, J.; Stellwagen, E. *Biochemistry* **1972**, *11*, 1195.

(22) Margoliash, E.; Frohwirt, N. *Biochem. J.* **1959**, *71*, 570.

(23) Tsong, T. Y. *Biochemistry* **1975**, *14*, 1542.

(24) Varhac, R.; Antalik, M. *Biochemistry* **2004**, *43*, 3564.